

Article

## Controlled Self-Assembly of Hexa-*peri*-hexabenzocoronenes in Solution

Jishan Wu, Andreas Fechtenkttter, Jrgen Gauss, Mark D. Watson,  
Marcel Kastler, Chrys Fechtenkttter, Manfred Wagner, and Klaus Mllen

*J. Am. Chem. Soc.*, **2004**, 126 (36), 11311-11321 • DOI: 10.1021/ja047577r • Publication Date (Web): 19 August 2004

Downloaded from <http://pubs.acs.org> on April 1, 2009

### More About This Article

---

Additional resources and features associated with this article are available within the HTML version:

- Supporting Information
- Links to the 14 articles that cite this article, as of the time of this article download
- Access to high resolution figures
- Links to articles and content related to this article
- Copyright permission to reproduce figures and/or text from this article

[View the Full Text HTML](#)



**ACS Publications**  
High quality. High impact.

## Controlled Self-Assembly of Hexa-*peri*-hexabenzocoronenes in Solution

Jishan Wu,<sup>†</sup> Andreas Fechtenkötter,<sup>†,§</sup> Jürgen Gauss,<sup>‡</sup> Mark D. Watson,<sup>†,||</sup>  
Marcel Kastler,<sup>†</sup> Chrys Fechtenkötter,<sup>†,⊥</sup> Manfred Wagner,<sup>†</sup> and Klaus Müllen\*<sup>†</sup>

Contribution from the Max Planck Institut für Polymerforschung, Ackermannweg 10,  
55128, Mainz, Germany, and Institut für Physikalische Chemie, Universität Mainz,  
55099 Mainz, Germany

Received April 27, 2004; E-mail: muellen@mpip-mainz.mpg.de

**Abstract:** Disc-shaped hexa-*peri*-hexabenzocoronenes (HBCs) peripherally substituted by flexible dodecyl chains (molecule **1**) or rigid polyphenylene dendrons (molecules **2a**, **b** and **3**) were efficiently synthesized. Steric hindrance arising from the substituents, from less hindered dodecyl to bulky dendrons, was utilized to program the self-assembly of the HBC cores in solution. The high tendency of the hexadodecyl-substituted HBC **1** to aggregate was determined by concentration and temperature-dependent <sup>1</sup>H NMR spectroscopic measurements and nonlinear least-squares analysis of the experimental data. The rigid dendrons in molecule **2a** suppress the  $\pi$ - $\pi$  interactions of the HBC cores to a certain extent, and a slow (with respect to the NMR time scale) monomer-dimer equilibrium is observed. This unique equilibrium was further controlled by temperature, concentration, and solvent to afford discrete monomeric or dimeric species. Further structural modifications such as the replacement of dodecyl groups in **2a** with hydrogen atoms resulted in a stable dimer structure in **2b** due to diminished steric hindrance, as supported by quantum chemical calculations. "Moving" the dendron arms closer to the HBC core gives molecule **3**, which exists only as a nonaggregated monomer. UV-vis absorption and fluorescence spectra of these discrete species revealed obvious differences in their electronic and optoelectronic properties which can be explained by the existence or absence of  $\pi$ - $\pi$  interactions.

### Introduction

$\pi$ - $\pi$ -Stacking interactions ubiquitously exist in nature<sup>1</sup> and are widely utilized by synthetic chemists to engineer complex supramolecular structures.<sup>2,3</sup> The nature of the  $\pi$ - $\pi$  interaction has been studied theoretically<sup>4</sup> and experimentally.<sup>5</sup> Recently, interest has developed in the use of  $\pi$ -stacks of conjugated  $\pi$ -systems as organic hole or electron conducting pathways in

organic electronic or optoelectronic devices.<sup>6</sup> For such processes, conformationally rigid and shape-persistent nanosized molecules, such as discotic liquid crystals<sup>2b,6,7</sup> and macrocycles,<sup>8</sup> have attracted great interest due to their excellent self-assembly and electronic properties. High one-dimensional charge carrier mobilities have been observed in discotic liquid crystalline materials based on phthalocyanines,<sup>9</sup> triphenylenes,<sup>10</sup> and hexa-*peri*-hexabenzocoronenes (HBCs).<sup>11</sup> Their  $\pi$ - $\pi$  interactions in

<sup>†</sup> Max Planck Institut für Polymerforschung.

<sup>‡</sup> Universität Mainz.

<sup>§</sup> Current address: Performance Chemicals, BASF, Aktiengesellschaft, E-EVD/MW - J550, 67056 Ludwigshafen, Germany.

<sup>||</sup> Current address: Department of Chemistry, University of Kentucky, Lexington, KY 40506-0055.

<sup>⊥</sup> Current address: Processing Engineering, BASF, Aktiengesellschaft, GCT/M - L540, 67056 Ludwigshafen, Germany.

- (1) (a) Saenger, W. *Principles of Nucleic Acid Structure*; Springer-Verlag: New York, 1984; pp 132–140. (b) Burley, S. K.; Petsko, G. A. *Adv. Protein Chem.* **1988**, *39*, 125–192. (c) Wakelin, L. P. G. *Med. Res. Rev.* **1986**, *6*, 275–340.
- (2) (a) Desiraju, G. R.; Gavezzotti, A. *J. Chem. Soc., Chem. Commun.* **1989**, 621–623. (b) Cammidge, A. N.; Bushby, R. J. In *Handbook of Liquid Crystals*; Demus, D., Goodby, J., Gray, G. W., Spiess, H. W., Vill, V., Eds.; Wiley-VCH: Weinheim, 1998; Vol. 2B, p 693. (c) Chandrasekhar, S. *Liq. Cryst.* **1993**, *14*, 3. (d) Adam, D.; Closs, F.; Frey, T.; Funhoff, D.; Haarer, D.; Ringsdorf, H.; Schuhmacher, P.; Siemensmeyer, K. *Phys. Rev. Lett.* **1993**, *70*, 457.
- (3) (a) Zimmerman, S. C.; VanZyl, C. M.; Hamilton, G. S. *J. Am. Chem. Soc.* **1989**, *111*, 1373–1381. (b) Ortholand, J. Y.; Slawin, A. M. Z.; Spencer, N.; Stoddart, J. F.; Williams, D. J. *Angew. Chem., Int. Ed. Engl.* **1989**, *28*, 1394–1395. (c) Askew, B.; Ballester, P.; Buhr, C.; Jeong, K. S.; Parris, K.; Williams, K.; Rebek, J. *J. Am. Chem. Soc.* **1989**, *111*, 1082–1090. (d) Shepodd, T. J.; Petti, M. A.; Dougerty, D. A. *J. Am. Chem. Soc.* **1988**, *110*, 1983–1985. (e) Diederich, F. *Angew. Chem., Int. Ed. Engl.* **1988**, *27*, 362–386.

- (4) (a) Hunter, C. A.; Sanders, J. K. M. *J. Am. Chem. Soc.* **1990**, *112*, 5525–5534. (b) Ravishanker, G.; Beveridge, D. L. *J. Am. Chem. Soc.* **1985**, *107*, 2565–2566. (c) Jorgensen, W. L.; Sererance, D. L. *J. Am. Chem. Soc.* **1990**, *112*, 4768–4777. (d) Linse, P. J. *J. Am. Chem. Soc.* **1992**, *114*, 4366–4373. (e) Hobza, P.; Selzle, L.; Schlag, E. W. *J. Am. Chem. Soc.* **1994**, *116*, 3500–3506. (f) Chipot, C.; Jaffe, R.; Maigret, B.; Pearlman, D. A.; Kollman, P. A. *J. Am. Chem. Soc.* **1995**, *117*, 11006–11010. (g) Janiak, C. *J. Chem. Soc., Dalton Trans.* **2000**, 3885–3896.
- (5) (a) Williams, J. H. *Acc. Chem. Res.* **1993**, *26*, 593–598. (b) Laatikainen, R.; Ratilainen, J.; Sebastian, R.; Santa, H. *J. Am. Chem. Soc.* **1995**, *117*, 11006–11010. (c) Cozzi, F.; Cinquini, M.; Annunziata, R.; Dwyer, T.; Siegel, J. S. *J. Am. Chem. Soc.* **1992**, *114*, 5729–5733. (d) Tucker, E. E.; Christian, S. D. *J. Phys. Chem.* **1979**, *83*, 426–427.
- (6) Bushby, R. J.; Lozman, O. R. *Curr. Opin. Solid State Mater. Sci.* **2002**, *6*, 569–578.
- (7) Chandrasekhar, S.; Prasad, S. K. *Contemp. Phys.* **1999**, *40*, 237–245.
- (8) (a) Moore, J. S. *Acc. Chem. Res.* **1997**, *30*, 402–413. (b) Höger, S. *J. Polym. Sci., Part A: Polym. Chem.* **1999**, *37*, 2685. (c) Haley, M. M. *Top. Curr. Chem.* **1999**, *201*, 81–130. (d) Bong, D. T.; Clark, T. D.; Granja, J. R.; Ghadiri, M. R. *Angew. Chem., Int. Ed.* **2001**, *40*, 988–1011.
- (9) (a) Bao, Z.; Lovinger, A. J.; Dodabalapur, A. *Adv. Mater.* **1997**, *9*, 42–44. (b) van de Craats, A. M.; Warman, J. M.; De Haas, M. P.; Adam, D.; Simmerer, J.; Haarer, D.; Schuhmacher, P. *Adv. Mater.* **1996**, *8*, 823.
- (10) Adam, D.; Schuhmacher, P.; Simmerer, J.; Häußling, L.; Siemensmeyer, K.; Etzsch, K. H.; Ringsdorf, H.; Haarer, D. *Nature* **1994**, *371*, 141–143.

solution<sup>12</sup> play an important role in promoting self-assembly in solid films, which is relevant for their electronic or optoelectronic properties.

Concentration and temperature-dependent UV–vis spectroscopy, <sup>1</sup>H NMR spectroscopy, and vapor pressure osmometry (VPO) have been used to study the self-assembly process of macrocycles,<sup>13</sup> which, in combination with a theoretical analysis, allowed the thermodynamic data ( $\Delta H$ ,  $\Delta S$ , and the association constant  $K$ ) during self-assembly to be elucidated.<sup>14</sup> In most cases, these molecules showed dynamic self-assembly in solution; that is, a polydisperse mixture of aggregates such as dimer, trimer, and larger aggregates existed with the distribution dependent on the concentration and temperature. The self-assembly could be further programmed for lower aggregates by introducing static charge repulsion<sup>12c</sup> or steric hindrance between the arms. Dendrimers were attached to the periphery of rigid cores such as phthalocyanines, leading to reduced association.<sup>15</sup> However, complete suppression of aggregation was unfulfilled by the use of flexible dendrons. An alternative that was explored was to introduce dendronized substituents to the axial position of phthalocyanine, resulting in nonaggregated monomer.<sup>16</sup>

While a discrete monomer–dimer self-assembly is a common phenomenon in protein dimerization,<sup>17</sup> such an equilibrium has rarely been observed in synthetic  $\pi$ -systems with  $\pi$ - $\pi$  interactions. Rapid (with respect to the NMR time scale) monomer–dimer equilibria have been observed in octahedral ruthenium and osmium complexes of heteroaromatic ligands via complementary  $\pi$ - $\pi$  pairing of the aromatic ligands.<sup>18</sup> The steric hindrance induced by the octahedral complex part limited the formation of higher aggregates. Cyclic alkynes containing three helicene units, 1,12-dimethylbenzo[*c*]phenanthrene, exhibited

a remarkable monomer–dimer association with obvious diastereoselectivity.<sup>19</sup> However, further control of monomer–dimer aggregation is needed to obtain slow equilibrium formation.

The unique materials properties of hexa-*peri*-hexabenzocoronene (HBC) and its derivatives have prompted extensive investigations.<sup>20</sup> Discotic liquid crystalline materials based on mesogens such as triphenylene,<sup>21</sup> porphyrin,<sup>22</sup> and phthalocyanine<sup>23</sup> display useful physical properties for application to organic electronics. HBCs possess a larger polycyclic aromatic hydrocarbon (PAH) core with strong intracolumnar  $\pi$ - $\pi$ -stacking interactions, and, as a result, alkyl- or alkylphenyl-substituted HBCs exhibit columnar mesophases with unusually high thermal stability, a high order parameter, and high one-dimensional charge carrier mobility.<sup>11,20</sup> These properties qualify HBCs as particularly promising candidates for organic semiconducting materials in field-effect transistors (FETs),<sup>24</sup> hole-conducting layers in photovoltaic devices or light-emitting diodes (LEDs),<sup>25</sup> and molecular wires in nanoscale molecular electronics.<sup>26</sup> The self-assembly of HBC-based materials in the bulk and at surfaces has been intensively studied by various techniques such as X-ray diffraction and scanning probe microscopy (SPM).<sup>27</sup> Film formation and order in the bulk state strongly suggest a study of the self-assembly of the discs in solution. The solution self-assembly behavior of a typical

- (11) (a) van de Craats, A. M.; Warman, J. M.; Müllen, K.; Geerts, Y.; Brand, J. D. *Adv. Mater.* **1998**, *10*, 36–38. (b) van de Craats, A. M.; Warman, J. M.; Fechtenkötter, A.; Brand, J. D.; Harbison, M. A.; Müllen, K. *Adv. Mater.* **1999**, *11*, 1469–1472.
- (12) (a) Schutte, W. J.; Sluyters-Rehbach, M.; Sluyters, J. H. J. *Phys. Chem.* **1993**, *97*, 6069–6073. (b) Parina, R. D.; Halko, D. J.; Swinehart, J. H. *J. Phys. Chem.* **1972**, *76*, 2343–2348. (c) Kadish, K. M.; Sazou, D.; Liu, Y. M.; Saoiabi, A.; Ferhat, M.; Guillard, R. *Inorg. Chem.* **1988**, *27*, 686–690. (d) Kano, K.; Fukuda, K.; Wakami, H.; Nishiyabu, R.; Pasternack, R. F. *J. Am. Chem. Soc.* **2000**, *122*, 7494–7502.
- (13) (a) Zhang, J. S.; Moore, J. S. *J. Am. Chem. Soc.* **1992**, *114*, 9701–9702. (b) Shetty, A. S.; Zhang, J. S.; Moore, J. S. *J. Am. Chem. Soc.* **1996**, *118*, 1019–1027. (c) Lahiri, S. L.; Thompson, J. L.; Moore, J. S. *J. Am. Chem. Soc.* **2000**, *122*, 11315–11319. (d) Höger, S.; Bonrad, K.; Mourran, A.; Beginn, U.; Möller, M. *J. Am. Chem. Soc.* **2001**, *123*, 5651–5659. (e) Tobe, Y.; Utsumi, N.; Kawabata, K.; Nagano, A.; Adachi, K.; Araki, S.; Sonoda, M.; Hirose, K.; Naemura, K. *J. Am. Chem. Soc.* **2002**, *124*, 5350–5364.
- (14) (a) Martin, R. B. *Chem. Rev.* **1996**, *96*, 3043–3064. (b) Horman, I.; Dreux, B. *Helv. Chem. Acta* **1984**, *67*, 754–764.
- (15) (a) Hecht, S.; Fréchet, J. M. J. *Angew. Chem., Int. Ed.* **2001**, *40*, 74–91. (b) Gorman, C. B.; Smith, J. C. *Acc. Chem. Res.* **2001**, *34*, 60–71. (c) Kimura, M.; Nakada, K.; Yamaguchi, Y.; Hanabusa, K.; Shirai, H.; Kobayashi, N. *Chem. Commun.* **1997**, 1215–1216. (d) Kernag, C. A.; McGrath, D. V. *Chem. Commun.* **2003**, 1048–1049. (e) Ng, A. C. H.; Li, X. Y.; Ng, D. K. P. *Macromolecules* **1999**, *32*, 5292–5298. (f) Brewis, M.; Helliwell, M.; McKeown, N. B.; Reynolds, S.; Shawcross, A. *Tetrahedron Lett.* **2001**, *42*, 813–816. (g) Kimura, M.; Shiba, T.; Yamazaki, M.; Hanabusa, K.; Shirai, H.; Kobayashi, N. *J. Am. Chem. Soc.* **2001**, *123*, 5636–5642.
- (16) (a) Brewis, M.; Clarkson, G. J.; Goddard, V.; Helliwell, M.; Holder, A.; McKeown, N. B. *Angew. Chem., Int. Ed.* **1998**, *37*, 1092–1094. (b) Brewis, M.; Clarkson, G. J.; Helliwell, M.; Holder, A. M.; McKeown, N. B. *Chem.-Eur. J.* **2000**, *6*, 4630–4636.
- (17) (a) Klemm, J. D.; Schreiber, S. L.; Crabtree, G. R. *Annu. Rev. Immunol.* **1998**, *16*, 569–592. (b) Shijder, H. J.; Ubarretxena-Belandia, I.; Blaauw, M.; Kalk, K. H.; Verheij, H. M.; Egmond, M. R.; Dekker, N.; Dijkstra, B. W. *Nature* **1999**, *401*, 717–721. (c) Korchuganov, D. S.; Nolde, S. B.; Reibarkh, M. Y.; Orekhov, V. Y.; Schulga, A. A.; Ermolyuk, Y. S.; Kirpichnikov, M. P.; Arseniev, A. S. *J. Am. Chem. Soc.* **2001**, *123*, 2068–2069. (d) Gamble, T. R.; Yoo, S.; Vajdos, F. F.; von Schwedler, U. K.; Worthylake, D. K.; Wang, H.; McCutcheon, J. P.; Sundquist, W. I.; Hill, C. P. *Nature* **1997**, *278*, 849–853.
- (18) (a) Ishow, E.; Gourdon, A.; Launay, J.-P. *Chem. Commun.* **1998**, 1909–1910. (b) Ishow, E.; Gourdon, A.; Launay, J.-P.; Chiorboli, C.; Scandola, F. *Inorg. Chem.* **1999**, *38*, 1504–1510. (c) Gut, D.; Rudi, A.; Kopilov, J.; Goldberg, I.; Kol, M. *J. Am. Chem. Soc.* **2002**, *124*, 5449–5456. (d) Bergman, S. D.; Reshef, D.; Groysman, S.; Goldberg, I.; Kol, M. *Chem. Commun.* **2002**, 2374–2375.
- (19) Nakamura, K.; Okubo, H.; Yamaguchi, M. *Org. Lett.* **2001**, *3*, 1097–1099.
- (20) (a) Watson, M.; Fechtenkötter, A.; Müllen, K. *Chem. Rev.* **2001**, *101*, 1267–1300. (b) Herwig, P.; Kayser, C.; Müllen, K.; Spiess, H. W. *Adv. Mater.* **1996**, *8*, 510–513. (c) Stabel, A.; Herwig, P.; Müllen, K. *Angew. Chem., Int. Ed. Engl.* **1995**, *34*, 1609–1611. *Angew. Chem.* **1995**, *107*, 335–339. (d) Fechtenkötter, A.; Saalwächter, K.; Harbison, M. A.; Müllen, K.; Spiess, H. W. *Angew. Chem., Int. Ed.* **1999**, *38*, 3039–3042. *Angew. Chem.* **1999**, *111*, 3224–3228. (e) Fechtenkötter, A.; Tchegotareva, N.; Watson, M.; Müllen, K. *Tetrahedron* **2001**, *57*, 3769–3783. (f) Samori, P.; Fechtenkötter, A.; Jäckel, F.; Böhme, T.; Müllen, K.; Rabe, J. P. *J. Am. Chem. Soc.* **2001**, *123*, 11462–11467. (g) Lee, M.; Kim, J.-W.; Peleshanko, S.; Larson, K.; Yoo, Y.-S.; Vaknin, D.; Markutsya, S.; Tsukruk, V. V. *J. Am. Chem. Soc.* **2002**, *124*, 9121–9128.
- (21) (a) Fontes, E.; Heiney, P. A.; de Jeu, W. H. *Phys. Rev. Lett.* **1988**, *61*, 1202–1205. (b) Gramsbergen, E. F.; Hoving, H. J.; de Jeu, W. H.; Praefcke, K.; Kohne, B. *Liq. Cryst.* **1986**, *1*, 397–400. (c) Rego, J. A.; Kumar, S.; Ringsdorf, H. *Chem. Mater.* **1996**, *8*, 1402–1409.
- (22) (a) Franck, B. *Angew. Chem., Int. Ed. Engl.* **1982**, *21*, 343–353. (b) Gregg, B. A.; Fox, M. A.; Bard, A. J. *J. Am. Chem. Soc.* **1989**, *111*, 3024–3029. (c) Shimizu, Y.; Miya, M.; Nagata, K.; Ohta, K.; Matsumura, A.; Yamamoto, I.; Kusabayashi, S. *Chem. Lett.* **1991**, 25–28. (d) Bahr, G.; Schleitzer, G. *Chem. Ber.* **1957**, *90*, 438–443. (e) Morelli, G.; Ricciardi, G.; Roviello, A. *Chem. Phys. Lett.* **1991**, *185*, 468–472.
- (23) (a) Pawlowski, G.; Hanack, M. *Synthesis* **1980**, 287–289. (b) Ohta, K.; Watanabe, T.; Tanaka, S.; Fujimoto, T.; Yamamoto, I.; Bassoul, P.; Kucharezyk, N.; Simon, J. *Liq. Cryst.* **1991**, *10*, 357–368. (c) Cuellar, E. A.; Marks, T. J. *Inorg. Chem.* **1981**, *20*, 3766–3770. (d) Ohta, K.; Watanabe, T.; Fujimoto, T.; Yamamoto, I. *J. Chem. Soc., Chem. Commun.* **1980**, 1611–1613.
- (24) van de Crass, A. M.; Stutzmann, N.; Bunk, O.; Nielsen, M. M.; Watson, M. D.; Müllen, K.; Chanzy, H. D.; Siringhaus, H.; Friend, R. H. *Adv. Mater.* **2003**, *15*, 495–499.
- (25) (a) Schmidt-Mende, L.; Fechtenkötter, A.; Müllen, K.; Moons, E.; Friend, R. H.; MacKenzie, J. *Science* **2001**, *293*, 1119–1122. (b) Tang, C. W. *Appl. Phys. Lett.* **1986**, *48*, 183. (c) Christ, T.; Glüsen, B.; Greiner, A. J.; Kettner, A.; Sander, R.; Stümpfen, V.; Tsukruk, V.; Wendorff, J. H. *Adv. Mater.* **1997**, *9*, 48–52. (d) Tang, C. W.; VanSlyke, S. A. *Appl. Phys. Lett.* **1987**, *51*, 913.
- (26) Martin, R. E.; Diederich, F. *Angew. Chem., Int. Ed.* **1999**, *38*, 1350–1377. *Angew. Chem.* **1999**, *111*, 1440–1469.
- (27) (a) Fischbach, I.; Pakula, T.; Minkin, P.; Fechtenkötter, A.; Müllen, K.; Spiess, H. W. *J. Phys. Chem. B* **2002**, *106*, 6408–6418. (b) Tchegotareva, N.; Yin, X.; Watson, M. D.; Samori, P.; Rabe, J. P.; Müllen, K. *J. Am. Chem. Soc.* **2003**, *125*, 9734–9739. (c) Ito, S.; Herwig, P.; Bohme, T.; Rabe, J. P.; Rettig, W.; Müllen, K. *J. Am. Chem. Soc.* **2000**, *122*, 7698–7706. (d) Samori, P.; Severin, N.; Simpson, C. D.; Müllen, K.; Rabe, J. P. *J. Am. Chem. Soc.* **2002**, *124*, 9454–9457. (e) Wu, J.; Watson, M. D.; Zhang, L.; Wang, Z.; Müllen, K. *J. Am. Chem. Soc.* **2004**, *126*, 177–186.

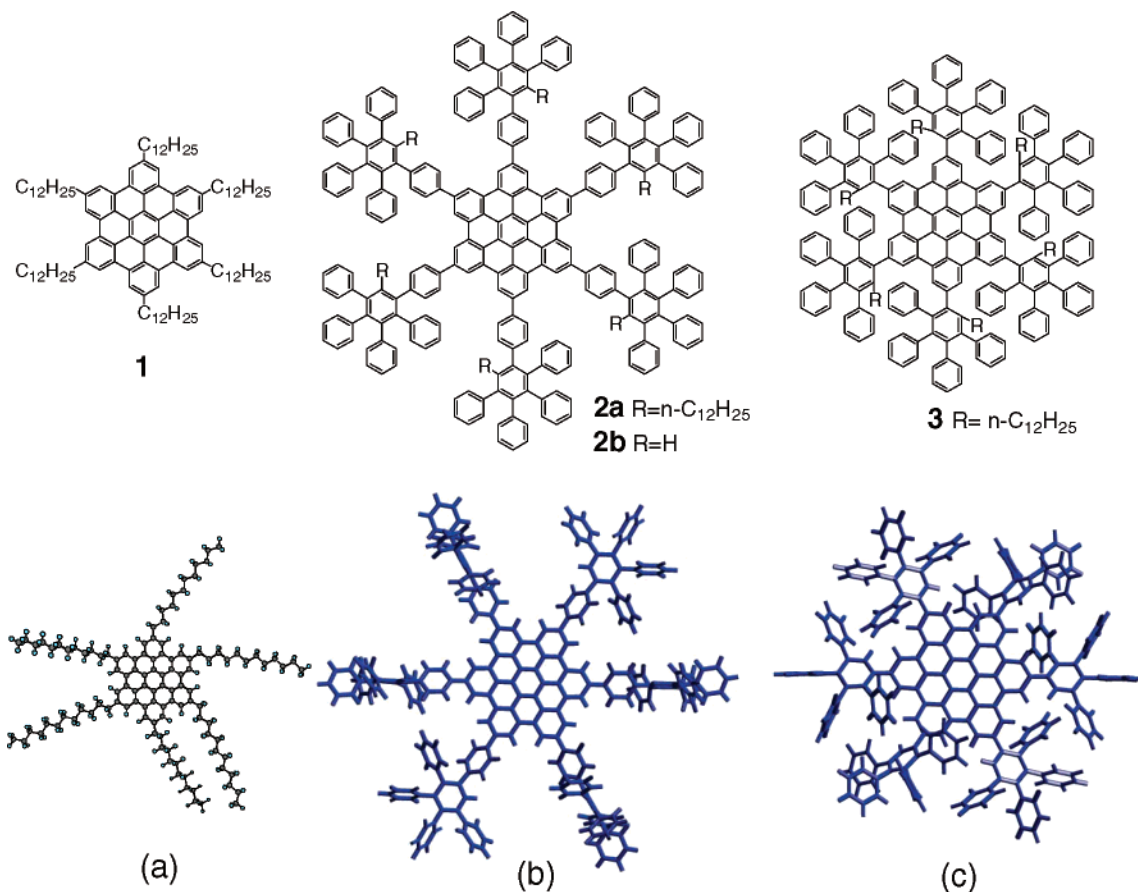


**Figure 1.** Molecular structures and three-dimensional models of the HBC molecules. Molecular mechanics energy minimization of **2a–b** and **3** was performed with Cerius 2 programs using the pcff 3.00 force field. The dodecyl groups in **2a** and **3** are omitted for clarity.

example, hexakis(4-dodecyl)-*peri*-hexabenzocoronene (**1** in Figure 1), has thus been investigated by standard  $^1\text{H}$  NMR spectroscopic methods in this Article. The aggregation of the discs has a great influence not only on their order, but also on the photophysical and electronic properties of each disc.<sup>28</sup> Less aggregated or isolated, nonaggregated HBCs are desirable to further understand structure–property relationships. Herein, shape-persistent, rigid polyphenylene dendrons<sup>29</sup> instead of flexible dendrimers have been peripherally attached to the HBC core in an attempt to modify the self-assembly of these discotic molecules. Thereby, the distance of the dendrons from the HBC core (compounds **2a**, **2b**, and **3** in Figure 1) and the nature of the substituents on the dendrons were varied. The self-assembly behavior of the title molecules in solution was studied by temperature- and concentration-dependent  $^1\text{H}$  NMR spectroscopy assisted by quantum chemical ab initio calculations. UV–vis and fluorescence spectroscopic measurements were conducted on these molecules under different conditions (concentrations and solvents) to disclose the effect of  $\pi$ – $\pi$  interactions.

## Synthesis

The hexadodecyl-substituted HBC, **1**, was synthesized according to our previous report.<sup>20c</sup> The dendronized HBCs, **2a,b**,

were synthesized using the insoluble, whereas highly reactive, building block hexakis(4-iodophenyl)-*peri*-hexabenzocoronene (**4**, Scheme 1) as already described by us.<sup>30</sup> The latter could be easily functionalized in suspension by six-fold Hagihara–Sonogashira coupling reactions to give soluble or insoluble HBC derivatives (**5a,b**) with nearly quantitative conversion. Subsequent Diels–Alder cycloaddition between the alkyne and tetraphenylcyclopentadienone afforded the desired compounds **2a,b** as soluble materials (Scheme 1).

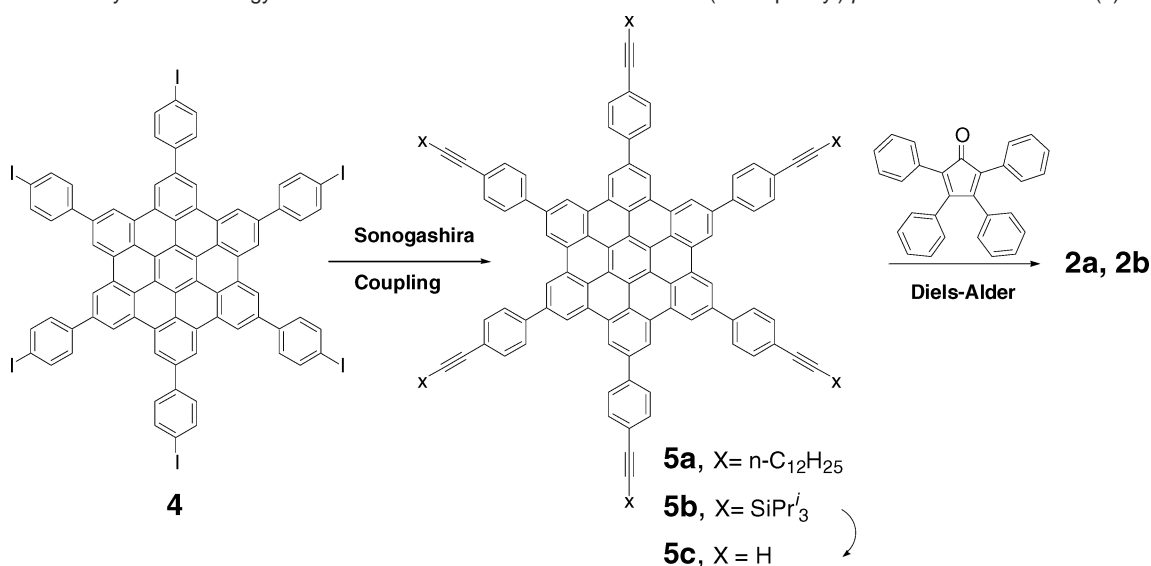
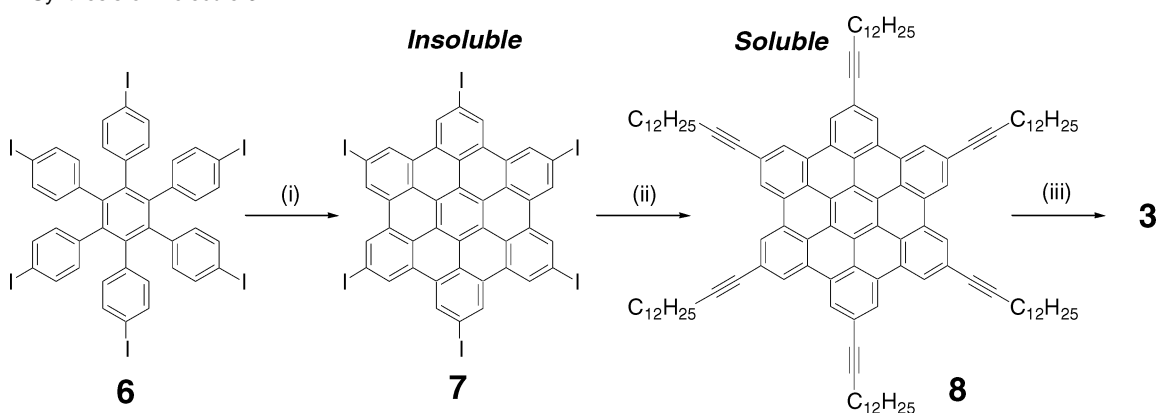
This synthetic strategy was also used to synthesize compound **3** as shown in Scheme 2. The insoluble HBC building block, hexakis(4-iodo)-*peri*-hexabenzocoronene (**7**), was successfully prepared by Lewis acid-mediated oxidative cyclodehydrogenation of the hexakis(4-iodophenyl)benzene (**6**).<sup>31</sup> The cyclodehydrogenation of hexakis(4-iodobiphenyl)benzene to afford hexakis(4-iodophenyl)-*peri*-hexabenzocoronene (**4**) was performed using iron trichloride over 1 h, whereas the complete fusion of **6** to HBC disc **7** under the same conditions took 24 h. This difference can be ascribed to the poor solubility of the targeted compound (**7**) and possibly to the electronic influence of the iodine atoms in the precursor (**6**). The analogous HBC building block, hexa(4-bromo)-*peri*-hexabenzocoronene, which carries the more electron-withdrawing bromines, was not accessible under similar cyclodehydrogenation conditions.<sup>27e</sup> The insoluble compound **7** was subjected to a six-fold Hagihara–Sonogashira coupling reaction with 1-tetradecyne, affording the

(28) (a) Bayer, A.; Hübner, J.; Kopitzke, J.; Oestreich, M.; Rühle, W.; Wendorff, J. H. *J. Phys. Chem. B* **2001**, *105*, 4596–4602. (b) Marguet, S.; Markovitsi, D.; Millié, P.; Sigal, H.; Kumar, S. *J. Phys. Chem. B* **1998**, *102*, 4697–4710. (c) Fleming, A. J.; Coleman, J. N.; Dalton, A. B.; Fechtenkötter, A.; Watson, M. D.; Müllen, K.; Byrne, H. J.; Blau, W. J. *J. Phys. Chem. B* **2003**, *107*, 37–43.

(29) (a) Wiesler, U.-M.; Weil, T.; Müllen, K. *Top. Curr. Chem.* **2001**, *212*, 2–40. (b) Berresheim, A. J.; Müller, M.; Müllen, K. *Chem. Rev.* **1999**, *99*, 1747.

(30) Wu, J.; Watson, M. D.; Müllen, K. *Angew. Chem., Int. Ed.* **2003**, *42*, 5329–5333.

(31) Hyatt, J. A. *Org. Prep. Proced. Int.* **1991**, *23*, 460–463.

**Scheme 1.** A New Synthetic Strategy for Dendronized HBC from Insoluble Hexakis(4-iodophenyl)-*peri*-hexabenzocoronene (**4**)<sup>30</sup>**Scheme 2.** Synthesis of Molecule **3**<sup>a</sup>

<sup>a</sup> (i) FeCl<sub>3</sub> (24 equiv)/CH<sub>3</sub>NO<sub>2</sub>, CH<sub>2</sub>Cl<sub>2</sub>, 24 h, 80–90%; (ii) 1-tetradecyne, Pd(PPh<sub>3</sub>)<sub>4</sub>, CuI, piperidine, 50 °C, 82%; (iii) tetraphenylcyclopentadienone, diphenyl ether, reflux, 26 h, 72%.

soluble HBC derivative **8** in 82% yield after chromatographic workup. The MALDI-TOF mass spectrum of **8** suggested the quantitative conversion without any deiodination during the reaction (see Supporting Information). The alkynes in compound **8** afford opportunities for further functionalizations. A six-fold Diels–Alder reaction between compound **8** and tetraphenylcyclopentadienone was then performed in refluxing diphenyl ether, and the HBC **3**, peripherally substituted with polyphenylene dendrons, was obtained. The MALDI-TOF mass spectroscopic characterization indicated complete six-fold Diels–Alder transformation despite the steric hindrance between the arms (Supporting Information). As becomes obvious from the molecular model in Figure 1, the core in **3** is surrounded by bulky rigid dendrons, and such a molecular arrangement is likely to suppress  $\pi$ – $\pi$  interaction between HBC discs.

### Self-Assembly of **1** in Solution Investigated by <sup>1</sup>H NMR Spectroscopy

The  $\pi$ – $\pi$  interactions of aromatic molecules lead to additional ring-current effects.<sup>4a</sup> As a result, the <sup>1</sup>H NMR spectra of aggregates are different from those of isolated monomeric species and are sensitive to concentration and temperature changes. A typical feature of the <sup>1</sup>H NMR spectra of compound

**1** is the significant line broadening and shielding due to the aggregation. Hence, concentration- and temperature-dependent <sup>1</sup>H NMR spectroscopy could be used to estimate the strength of the self-assembly (association constant *K*) and thermodynamics ( $\Delta H$  and  $\Delta S$ , respectively) of aromatics.<sup>14</sup>

The <sup>1</sup>H NMR spectra of compound **1** in *d*<sup>4</sup>-tetrachloroethane were recorded over a range of temperatures and concentrations. On heating from 60 to 120 °C, the aromatic signals assigned to the HBC core shift downfield by 0.26 ppm (from  $\delta = 8.1$  ppm to  $\delta = 8.4$  ppm, Supporting Information). A less pronounced downfield shift can be observed for the  $\alpha$ -CH<sub>2</sub> protons of the dodecyl chains. Likewise, a decrease in the concentration from  $51.16 \times 10^{-3}$  to  $1.35 \times 10^{-3}$  M at constant temperature (60 °C) results in a downfield shift by almost 0.5 ppm as shown in Figure 2. Such a temperature and concentration dependence is commonly observed for other disc-like aromatic systems.<sup>12,13</sup> In a face-to-face aggregate of the discs, the protons of one molecule are localized in the secondary magnetic field of the neighboring aromatics, resulting in a shielding, and such a shielding effect depends on the size of the aggregates. Because the size of the aggregates in solution decreases at higher temperature and lower concentrations, a deshielding effect is observed in the NMR spectra. Dilution of the solution to 1.63

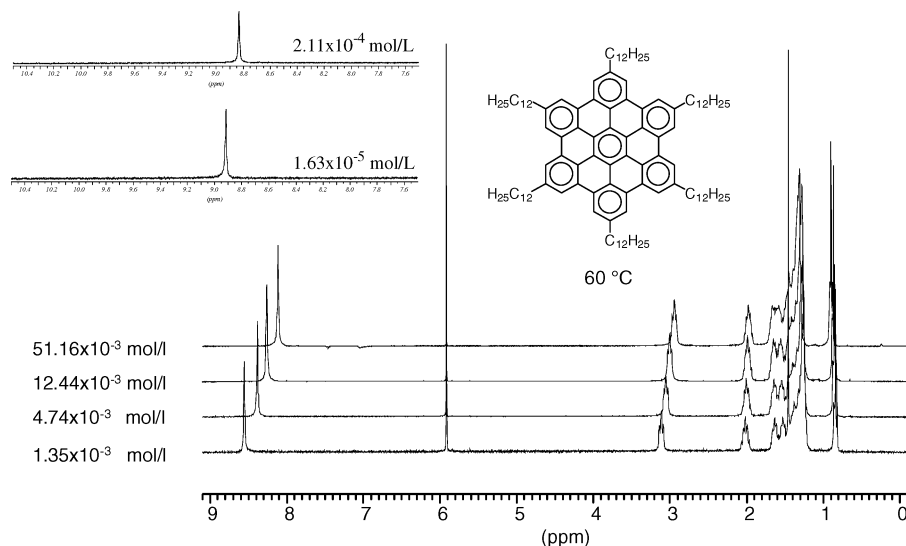


**Figure 2.** Concentration-dependent  $^1\text{H}$  NMR measurements of **1** in  $\text{D}^4$ -1,1,2,2-tetrachloroethane at  $60\text{ }^\circ\text{C}$ .

$\times 10^{-5}$  M yields a single resonance peak at 8.9 ppm. The  $^1\text{H}$  NMR spectroscopic characterization of more dilute solutions was limited by the probe sensitivity.

The experimentally determined NMR shifts as a function of the concentration of the HBC were used in the self-assembly models to estimate the association constants.<sup>14a</sup> Here, four models were used, and the constants in the models were fitted to experimental data using nonlinear least-squares fitting. All models are based on the assumption that the chemical shift of an aggregate can be expressed in terms of those of the monomer, a molecule at the end of a stack, and a molecule within a stack, and their respective concentrations. The equal K (EK) model assumes that the addition of a molecule to a stack occurs with the same equilibrium constant as other molecules. The attenuated K (AK) model assumes that successive additions became less probable and equilibrium constants taper off. These models assume that only nearest-neighbor interactions produce chemical shifts and they can be extended to account for the interactions of next-nearest-neighbors (EKNN and AKNN, respectively). A graphical fit of the data and a summary of parameters determined using the different models for the curve-fitting are given in Figure 3 and Table 1, respectively. The experimental data agree well with the fitting. The association constants range from 188 to  $457\text{ M}^{-1}$ . These values are much higher than those of macrocycles<sup>13,19</sup> in similar solvents because of the large  $\pi$ - $\pi$  overlap between the HBC cores. The aggregation behavior of discotic liquid crystalline phthalocyanines was also investigated in a similar approach by Schutte and co-workers.<sup>12a</sup> The equilibrium constants obtained by them in dodecane at room temperature are much higher than the data presented here, but this difference in magnitude certainly can be explained by several reasons; the elevated temperature utilized in this experiment (according to the van't Hoff law), the more polar solvent selected here (for solubility reasons), and the highly simplified model used by them where higher aggregates are neglected. The fitted graph crosses the y-axis at around 9.0 ppm, which is below the determined chemical shift for the lowest concentration used in the calculations, suggesting that the NMR chemical shift of the monomer ( $P_\alpha$ ) is around 9.0 ppm. Recently, quantum chemical ab initio methods such as Hartree-Fock (HF) and density functional theory (DFT) were used to compute the

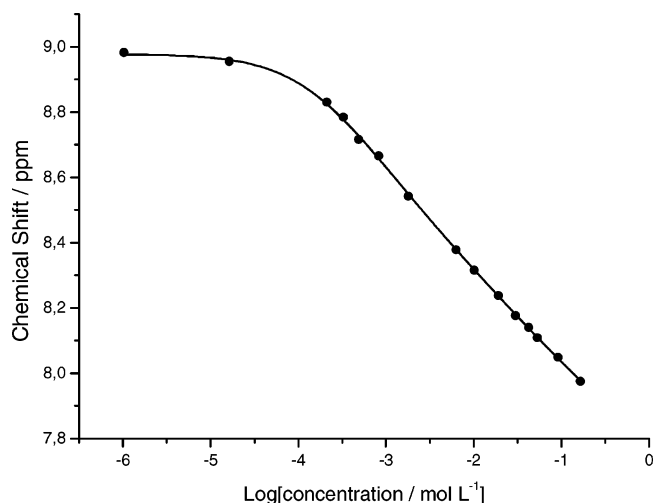


**Figure 3.** Curve fitting by nonlinear least-squares analysis of the concentration-dependent  $^1\text{H}$  NMR experimental data.

geometry and the NMR chemical shifts of large polycyclic aromatic compounds, and a  $^1\text{H}$  NMR chemical shift of 9.5 ppm was estimated for the protons of the HBC core of hexakis(4-methyl)-*peri*-hexabenzocoronene.<sup>32</sup> Herein, the 0.5 ppm deviation between the experiment and calculation could arise from shortcomings of the used methods, from neglect of vibrational effects, and from solvent effects not considered in the calculations.

The above experimental results highlight the tendency of HBC materials to self-assemble in solution and explain the high order of HBC materials in spin-coated or drop-casted films prepared from solution.

### Self-Assembly of Dendronized HBC **2a**, **2b**, and **3** in Solution

The temperature-dependent  $^1\text{H}$  NMR spectra of **2a** in  $\text{D}^4$ -1,1,2,2-tetrachloroethane (5 mg/mL) are shown in Figure 4. Two sets of resonances were observed: one labeled with a star (\*) and another with a square (■), corresponding to two independent

(32) (a) Ochsenfeld, C.; Brown, S. P.; Schnell, I.; Gauss, J.; Spiess, H. W. *J. Am. Chem. Soc.* **2001**, *123*, 2597–2606. (b) Ochsenfeld, C. *Phys. Chem. Chem. Phys.* **2000**, *2*, 2153–2159.

**Table 1.** Parameters for the Different Models Using the Entire Set of Experimental Data<sup>a</sup>

| EK model               | AK model               | EKNN model             | AKNN model             |
|------------------------|------------------------|------------------------|------------------------|
| $K_E = 188.68$ L/mol   | $K_A = 457.32$ L/mol   | $K_E = 188.66$ L/mol   | $K_A = 457.39$ L/mol   |
| $\rho = 4.485$         | $\tau = 3.834$         | $\rho = 4.485$         | $\tau = 3.834$         |
| $f = 0.4970$           | $f = 0.3773$           | $r = 0.005954$         | $r = 0.3253$           |
| $P_\alpha = 8.977$ ppm | $P_\alpha = 8.978$ ppm | $P_\alpha = 8.977$ ppm | $P_\alpha = 8.978$ ppm |
| $P_\xi = 7.641$ ppm    | $P_\xi = 7.239$ ppm    | $P_\xi = 7.641$ ppm    | $P_\xi = 7.239$ ppm    |

<sup>a</sup>  $K_E$ , equilibrium constant;  $K_A$ , association constant;  $\rho$ , factor by which dimer formation differed from larger aggregate formation in EK models ( $K_2 = \rho K_E$ );  $\tau$ , factor by which dimer formation differed from larger aggregate formation in AK models ( $K_2 = \tau K_A/2$ );  $f$ , factor relating the shift of the terminal molecule in the aggregate to that of the monomer and the interior molecule ( $P_\lambda = (1 - f)P_\alpha + fP_\xi$ );  $r$ , factor indicating the effect of the next-nearest-neighbor;  $P_\alpha$ , NMR chemical shift of monomer;  $P_\xi$ , NMR chemical shift of the interior molecule. Detailed explanations of these models were presented in ref 14a.

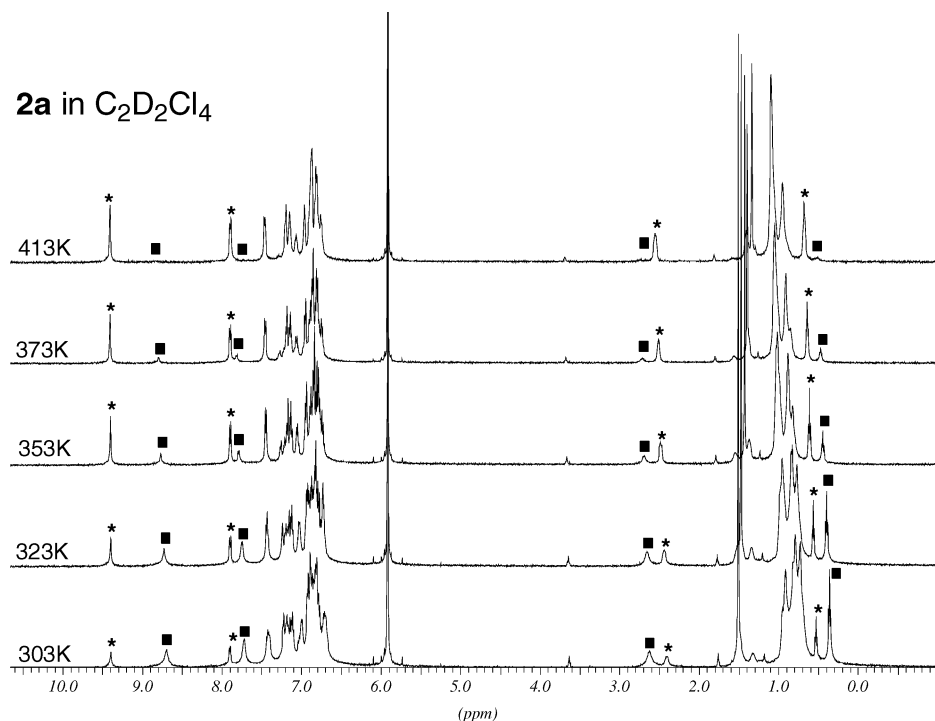


**Figure 4.** Temperature-dependent <sup>1</sup>H NMR spectra of **2a** in D<sup>4</sup>-1,1,2,2-tetrachloroethane (5 mg/mL). Two sets of independent resonances were labeled by a star (\*) and a square (■), respectively.

species. Upon heating from 303 to 413 K, the intensity ratio of the downfield resonances (\*) and the upfield species (■) increased to the point where at 413 K only one species (\*) was observed. The room-temperature resonances of the protons of the HBC core were located at about 9.4 and 8.7 ppm. Upon increasing the temperature from 303 to 413 K, the high-field resonance shifted slightly to lower field by about 0.12 ppm; however, the downfield resonance remained essentially unchanged. A similar trend was noted for all pairs of signals (in particular, those within the aromatic region). Given the temperature independence of the resonances (\*), this species can be safely assigned as the nonaggregated monomer of molecule **2a** in agreement with the quantum chemical calculations (see below). The dodecyl chains in the monomer of molecule **2a** were strongly shielded with respect to free-rotating alkyl chains. For example, the resonances assigned to the terminal methyl groups lie at 0.55 ppm at room temperature due to the shielding of alkyl chains by the polyphenylene dendrons (see the molecular model in Figure 1), and, at 413 K, the increased mobility of the alkyl chains deshields the dendrons.

The HBC core peak at 8.7 ppm appeared upfield by 0.7 ppm relative to the monomer and was assigned to an aggregated HBC species (labeled with a square), again in agreement with the

calculations (see below). The resonances for the aromatic phenylene rings and long alkyl chains are also strongly shifted to high field, the only exception being the resonances around 2.5 ppm assigned to the  $\alpha$ -CH<sub>2</sub> of the dodecyl chain at the bay position which have the opposite tendency. The observed shift to lower field of the resonances in the aggregate of **2a** with increased temperature can be explained by the slight increase of the  $\pi$ - $\pi$  distance during the heating or by a decrease of the size of the aggregate.

Concentration-dependent <sup>1</sup>H NMR spectroscopic studies of compound **2a** were also conducted in D<sup>4</sup>-1,1,2,2-tetrachloroethane as shown in Figure 5. Again, two sets of resonances were assigned to two independent species, one labeled with a star (\*, monomer) and another labeled with a square (■, aggregate). The intensity ratio of the corresponding monomer and aggregate signals gradually decreased when increasing the concentration from  $3.32 \times 10^{-5}$  to  $7.63 \times 10^{-4}$  M (Figure 5). The NMR chemical shifts for each species (the monomer and the aggregate), however, remained constant. This phenomenon suggests that the aggregated species is a discrete rather than a multidispersed aggregate.

To further understand the aggregate species, quantum chemical calculations on the geometry and NMR chemical shifts were

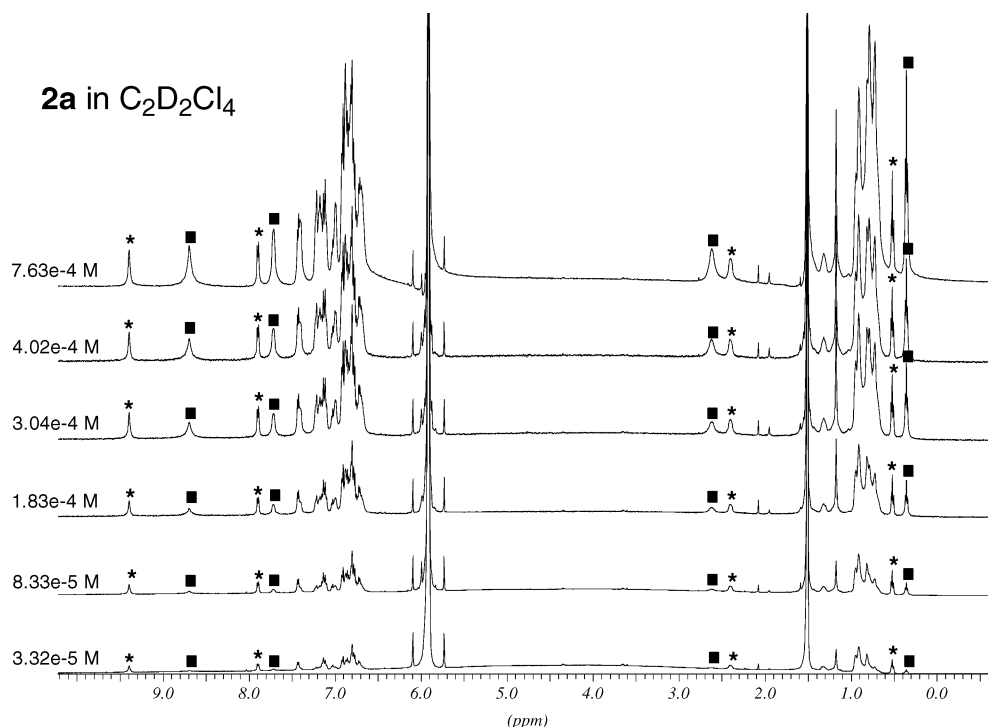


**Figure 5.** Concentration-dependent  $^1\text{H}$  NMR spectra of **2a** in  $\text{D}^4$ -1,1,2,2-tetrachloroethane at room temperature. Two sets of independent resonances are labeled by a star (\*) and a square (■), respectively.

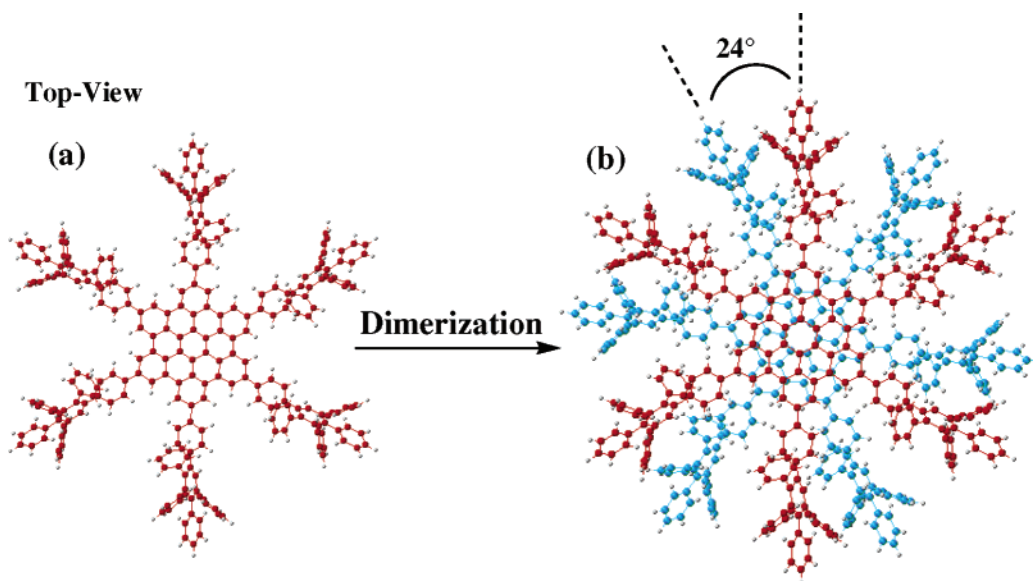


**Figure 6.** Quantum chemically (at the RI-DFT/SV(P) level) calculated monomer and ideal dimer structures of **2b**.

performed for a monomer and a dimer structure of **2a**.<sup>33</sup> The dodecyl substituents in molecule **2a** were omitted to simplify the calculations given the large molecular size; that is, the calculations were conducted for molecule **2b**. First, the geometry optimization for the monomer of **2b** was achieved at the RI-DFT level<sup>34</sup> assuming that the molecules possess a six-fold symmetry ( $C_6$  symmetry) with all of the dendrons being tilted in the same direction. The optimized structure of the monomer of molecule **2b** (420 atoms, 4422 basis functions) is shown in Figure 6a. Rotation of the phenyl rings about the bridged-head carbon–carbon single bond leaves some space between the

dendron arms, allowing another molecule, after a slight rotation, to approach from the axial direction to form a dimer structure. Other stacking motifs including, for example, an edge-on geometry<sup>4a</sup> were disregarded because the reduced symmetry would lead to multiple resonances for the protons of the HBC core; however, only one resonance signal was observed experimentally. A possible structure for the dimer was investigated at the RI-DFT/SV(P) level (840 atoms, 7872 basis functions). Optimization was only carried out with respect to

(33) All of the calculations have been carried out using the TURBOMOLR program package. Ahlrichs, R.; Bär, M.; Häser, M.; Horn, H.; Kölmel, C. *Chem. Phys. Lett.* **1989**, *162*, 165.

(34) (a) Koch, W.; Holthausen, M. *A Chemist's Guide to Density Functional Theory*; Wiley-VCH: Weinheim, 2000. (b) Parr, R.; Yang, W. *Density-Functional Theory of Atoms and Molecules*; Oxford University Press: New York, 1989. (c) Eichkorn, K.; Treutler, O.; Öhm, H.; Häser, M.; Ahlrichs, R. *Chem. Phys. Lett.* **1995**, *240*, 283. (d) Schäfer, A.; Horn, H.; Ahlrichs, R. *J. Chem. Phys.* **1992**, *97*, 2571.



the rotational angle of the second molecule with respect to the first one, while the structures of the individual monomers were kept frozen and the distance of the two molecules was fixed to 3.5 Å. The optimization procedure yielded an angle of about 24°; the corresponding dimer model is presented in Figure 6b. The dendrons in one HBC molecule fit well into the free space between the dendron arms of the second HBC molecule, forming an interlocked face-to-face stacked dimer structure without any steric overcrowding. Larger face-to-face stacks, even with the HBC rotating by some angle about the stacking axis, are precluded due to steric hindrance induced by the rigid, bulky dendron arms as revealed by simple molecular model calculations. Therefore, the unique association behavior of molecule **2a** actually is a monomer–dimer equilibrium.

The <sup>1</sup>H NMR chemical shifts for the monomer of molecule **2b** were calculated at the HF/3-21G<sup>35</sup> level based on the above-optimized structure, and a value of 10.2 ppm for the HBC core protons was obtained. As the corresponding calculations for the dimer are time-demanding, model calculations for a hexa(4-biphenyl)-*peri*-hexabenzocoronene dimer were instead performed. Because the calculations for the corresponding monomer yielded essentially identical chemical shifts for the HBC protons as for the **2b** monomer, this was assumed to be a realistic model for the **2b** dimer. Two chemical shift values at 9.45 and 9.70 ppm were thus obtained. Assuming a systematic error of about 0.5 ppm for the HF/3-21G calculations (based on calculations for the parent system), this yields a corrected value of about 9.7 ppm in good agreement with the experimental value of 9.4 ppm for **2a**. The discrepancy of ca. 0.6 ppm between calculated and experimental shift is again mainly attributed to a systematic error in the calculations, and the corrected values of about 8.9–9.1 ppm are in satisfactory agreement with the value attributed to the dimer of **2a**. Maybe more important, the computed chemical shift difference between monomer and dimer of 0.68 ppm is close to the actual experimental difference of 0.7 ppm found for **2a**.

The self-assembly of **2a** can be further controlled by the choice of the solvent. In a nonpolar solvent such as cyclohexane, only one set of resonances assigned to the dimer was observed. Addition of carbon disulfide (a good solvent for polycyclic aromatic hydrocarbons) to the solution led to the coexistence of monomer and dimer, and eventually to the exclusive existence of the monomer when excessive CS<sub>2</sub> was added. Similarly, only the monomer was detected in 1,2,4-trichlorobenzene (TCB) or 1,2-dichlorobenzene (DCB) at low concentrations (around 10<sup>-6</sup> M).

This monomer–dimer self-assembly was further evidenced by the dynamic light-scattering (DLS) measurements. For example, only very small particles with diameters around 1.4 nm are detected in a cyclohexane solution of **2a** (1 mg/mL, at which only a dimer existed), indicating no higher HBC–HBC  $\pi$ -stacking exists. The DLS measurements of **2a** in carbon disulfide or 1,2,4-trichlorobenzene in which monomer can be obtained in suitable concentration, however, were not successful. This was due to the low contrast in the refractive index between the solvents and the HBC molecules and, at the same time, the small particle size lying on the limit of DSL methods.

The appearance of two sets of NMR resonances instead of averaged signals, which are sensitive to changes of temperature, concentration, and solvent, suggests that the self-assembly process is slow on the NMR time scale. It is worthwhile to mention that such slow self-assembly processes are found for natural protein folding, but are seldom observed in synthetic nonbiological macromolecules.<sup>17</sup> Moore et al. disclosed that the *meta*-oligophenyleneethynyls could fold into a helical conformation under the influence of solvophobic forces and this mimics the behavior of biopolymers.<sup>36</sup> The facial stacking of compound **2a** represents another unique nonbiological example of solution phase, reversible self-assembly.

Replacement of the dodecyl groups (**2a**) with hydrogen atoms (**2b**) was expected to diminish the steric hindrance in the dimerization process. According to the temperature-dependent <sup>1</sup>H NMR spectra of **2b** in D<sup>4</sup>-1,1,2,2-tetrachloroethane (Figure 7), only one set of resonances was observed. The resonance at about 8.7 ppm (\*) was assigned to protons of the HBC core. Given the significant upfield shift of all of the resonances with respect to that of monomer of **2a** as well as the above results of the calculations, these resonances were assigned to an aggregated dimer structure of **2b**. This conclusion is supported by concentration-dependent <sup>1</sup>H NMR spectra, in which almost no change in the chemical shifts was observed over a range of concentrations (Supporting Information). The slight downfield shift of the resonance with increasing temperature, as observed for the dimer of **2a**, can be explained by a small change in the HBC–HBC distance with the temperature. The dimer structure was stable even upon addition of carbon disulfide. This stronger association of **2b** relative to **2a** can be ascribed to the diminished steric hindrance in the former and more efficient interlocking of the polyphenylene dendrons.

Further structural modification of the HBC such as attachment of the dendrons closer to the HBC core led to the distorted molecule **3**. The bulky substituents totally suppressed the aggregation of the HBC core and, at the same time, gave rise to a complex mixture of conformational isomers as disclosed by the temperature-dependent <sup>1</sup>H NMR spectra (Figure 8). Multiple resonances for the HBC core protons were observed even at temperatures up to 140 °C. In **3**, the rotation of dendrons about the carbon–carbon bonds that connect the HBC core and the dendrons is restricted due to the steric hindrance arising from the alkyl chains as well as the neighboring dendrons. Thus, the multiple resonances can be explained by the existence of conformers; the shape and relative intensity of the signals change slightly with temperature, a consequence of the temperature-induced conformational transformations. The resonances at about 8.7 ppm (\*) can be assigned to the protons of the HBC core, while a more detailed analysis of the conformational isomers is not possible due to the overlap of the complex resonances.

## Optical Spectra

The spontaneous formation of molecular assemblies via  $\pi$ – $\pi$  interaction in solution or in the condensed state is a characteristic feature of the alkyl- and alkylphenyl-substituted HBCs.<sup>27a,c</sup> Such interactions strongly affect the electronic states and, thus, the

(35) (a) Wolinski, K.; Hinton, J. F.; Pulay, P. *J. Am. Chem. Soc.* **1990**, *112*, 8251. (b) Häser, M.; Ahlrichs, R.; Baron, H. P.; Weis, P.; Horn, H. *Theor. Chim. Acta* **1992**, *83*, 455. (c) Binkley, J. S.; Pople, J. A.; Hehre, W. J. *J. Am. Chem. Soc.* **1980**, *102*, 939.

(36) (a) Nelson, J. C.; Saven, J. G.; Moore, J. S.; Wolynes, P. G. *Science* **1997**, *277*, 1793–1796. (b) Prince, R. B.; Saven, J. G.; Wolynes, P. G.; Moore, J. S. *J. Am. Chem. Soc.* **1999**, *121*, 3114–3121. (c) Brunsveld, L.; Meijer, E. W.; Prince, R. B.; Moore, J. S. *J. Am. Chem. Soc.* **2001**, *123*, 7978–7984. (d) Oh, K.; Jeong, K. S.; Moore, J. S. *Nature* **2001**, *414*, 889–893.

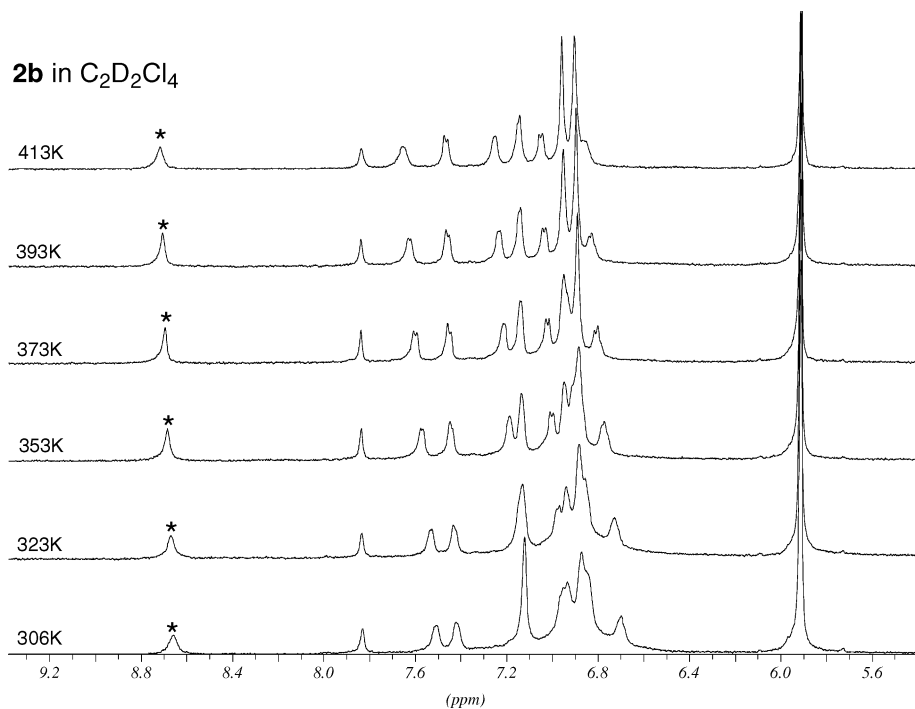


**Figure 7.** Temperature-dependent  $^1\text{H}$  NMR spectra of **2b** in  $\text{D}^4$ -1,1,2,2-tetrachloroethane (3 mg/mL).

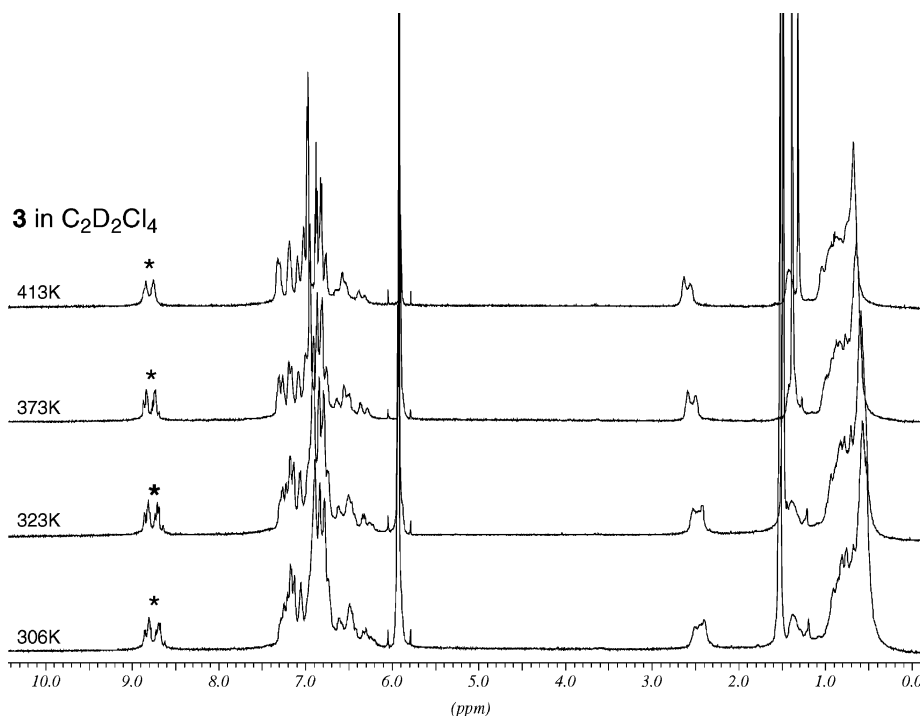


**Figure 8.** Temperature-dependent  $^1\text{H}$  NMR spectra of **3** in  $\text{D}^4$ -1,1,2,2-tetrachloroethane (3 mg/mL).

absorption and emission spectra.<sup>28</sup> The photophysical properties of **1** have been studied by steady-state and time-resolved spectroscopy. Due to aggregation, both absorption and emission bands changed as a function of concentration, and a multi-exponential rather than monoexponential fluorescence decay of **1** in solution was observed.<sup>37</sup> Because optimal conditions can be selected for discrete monomer or dimer assemblies, it is of interest to study their photophysical properties under differ-

ent conditions using UV-vis absorption and fluorescence spectroscopy.

The UV-vis absorption spectra of **2a**, **2b**, and **3** in different solvents and concentrations carefully chosen to give a discrete monomer (**2a** in 1,2,4-trichlorobenzene and  $\text{CS}_2$ , **3** in 1,2,4-trichlorobenzene) and dimer (**2a** in cyclohexane, **2b** in 1,2-dichlorobenzene) are shown in Figure 9a. The monomer of **2a** has a band structure very similar to that of **3**; however, the absorption maximum (*p*-band) is red-shifted by 12 nm from 373 nm in **3** to 385 nm in **2a**. Recalling that the absorption

(37) Biasutti, M. A.; Rommens, J.; Vacs, A.; Feyter, S. De.; De Schryver, F. D.; Herwig, P.; Müllen, K. *Bull. Soc. Chim. Belg.* **1997**, *106*, 659–664.

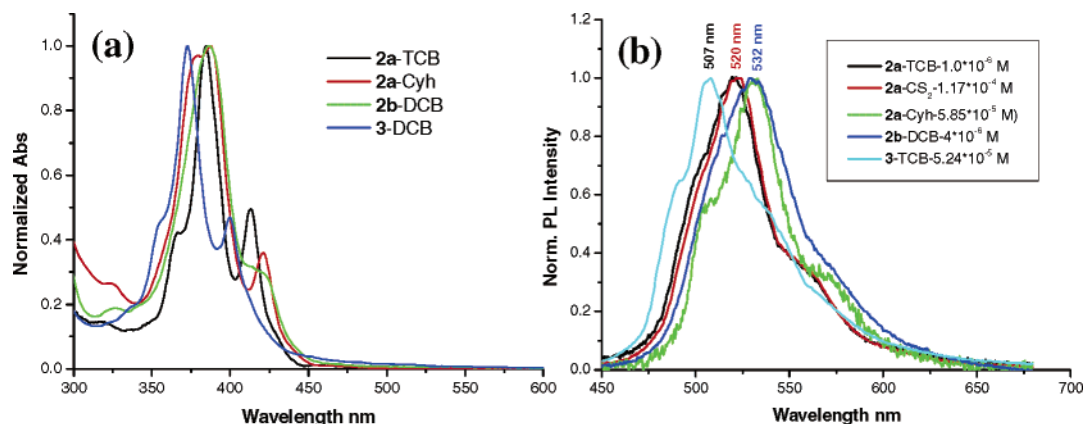


**Figure 9.** Normalized UV–vis absorption spectra and fluorescence spectra of **2a**, **2b**, and **3** for different solvents and concentrations. The following solutions were used: **2a** in 1,2,4-trichlorobenzene ( $1.0 \times 10^{-6}$  M), **2a** in carbon disulfide ( $1.17 \times 10^{-4}$  M), **2a** in cyclohexane ( $5.85 \times 10^{-5}$  M), **2b** in 1,2-dichlorobenzene ( $4 \times 10^{-6}$  M), and **3** in 1,2,4-trichlorobenzene ( $5.24 \times 10^{-5}$  M).

maximum of compound **1** in chloroform is at 360 nm, the red-shift of the absorption band upon going from **1** to **3** and **2a** can be ascribed to extended conjugation between the dendrons and HBC core, and the blue-shift of **3** with respect to **2a** can be ascribed to a more distorted conformation in molecule **3**. The absorption band of **2a** as a dimer species in cyclohexane was strongly influenced by the  $\pi$ – $\pi$  interaction of the HBC cores. The pronounced shoulder band at 366 nm in the monomer is red-shifted to 379 nm in the dimer, and the  $p$ -band at the maximum as well as the  $\beta$ -band at longer wavelength (413 nm in the monomer) were also red-shifted by 3 and 8 nm, respectively. While theoretical and experimental work has revealed that the cofacial stacking of aromatic  $\pi$ -systems could lead to a blue-shift of the absorption band with respect to the nonaggregated state,<sup>38</sup> here the dimerization of the dendronized HBC involves not only cofacial  $\pi$ -stacking but also the coaxial rotation of the discs, with the possibility of electronic interactions between the rigid dendrons and conformational changes during the association process or after photoexcitation. A similar band change was found in the dimer of molecule **2b**, which displayed a broadened absorption band centered at 387 nm and a weak  $\beta$ -band (shoulder) at about 421 nm. The obvious changes in the UV–vis absorption spectra between the HBC monomer and dimer structure can be regarded as the consequence of  $\pi$ – $\pi$  interactions between the HBC cores in the dimer.

The normalized fluorescence spectra of **2a**, **2b**, and **3** with the same solutions as described above for the UV–vis spectroscopic measurements are shown in the Figure 9b. While the monomer of **2a** in CS<sub>2</sub> and 1,2,4-trichlorobenzene had almost identical emission spectra with maximum emission at 520 nm, the dimer of **2a** in cyclohexane displayed an obvious bathochromic emission at 532 nm. This is typical of assemblies of conjugated  $\pi$ -system due to excimer formation or migration of photogenerated species to low-energy domains of the samples.<sup>39</sup> The dimer of **2b** in 1,2-dichlorobenzene showed an emission similar to that of the dimer of **2a** with a maximum at 532 nm. On the other hand, **3** displayed a blue-shifted emission band at around 507 nm with a well-resolved structure.

In summary, the controlled monomer and dimer structures of the dendronized HBCs **2a**, **2b**, and **3** in solution exhibited different photophysical properties such as band structure and absorption or emission wavelength. All of these differences can be adequately explained by the existence or absence of the  $\pi$ – $\pi$  interactions between the HBC cores in the unique monomer–dimer equilibrium.

## Conclusion

The solution self-assembly behavior of the hexa-*peri*-hexabenzocoronene (HBC) was programmed by the appropriate choice of peripheral substituents. HBCs with either flexible alkyl chains (molecule **1**) or rigid polyphenylene dendrons (**2a**, **2b**, and **3**) were synthesized following a new synthetic strategy. The hexadodecyl-substituted HBC **1** displayed a high tendency to aggregate in solution as disclosed by concentration- and temperature-dependent <sup>1</sup>H NMR spectroscopy. The rigid dendron arms in molecule **2a** suppressed the  $\pi$ -stacking to some extent and resulted in a unique monomer–dimer equilibrium, which was slow on the NMR time scale and could be controlled by temperature, concentration, and solvent. The replacement of the dodecyl chains in **2a** with hydrogen atoms yielded the dendronized molecule **2b**, which exhibited a stable dimerized structure due to diminished steric hindrance. Further structural modification such as “moving” the dendron arms closer to the HBC core gives molecule **3**, which only exists as a nonaggregated monomer. The UV–vis absorption and fluorescence spectroscopic measurements of these discrete monomer and dimer species revealed the effect of the  $\pi$ – $\pi$  interaction between the aromatic discs.

This study of the controlled self-assembly of HBC molecules in solution shows how structural and environmental factors can affect the supramolecular behavior and electronic properties of disc-shaped  $\pi$ -systems. The extremely slow monomer–dimer equilibrium of **2a** is rarely observed in synthetic nonbiological

(38) (a) Cornil, J.; dos Santos, D. A.; Beljonne, D.; Shuai, Z.; Brédas, J. L. In *Semiconducting Polymers*; Hadziioannou, G., van Hutten, P. F., Eds.; Wiley–VCH: Weinheim, 2000; pp 88–114. (b) Lewis, F. D.; Wu, T.; Burch, E. L.; Bassani, D. M.; Yang, J. S.; Schneider, S.; Jäger, W.; Letsinger, R. L. *J. Am. Chem. Soc.* **1995**, *117*, 8785–8792. (c) Liang, K.; Farahat, M. S.; Perlstien, J.; Law, K. Y.; Whitten, D. G. *J. Am. Chem. Soc.* **1997**, *119*, 830–831.

(39) (a) Lemmer, U.; Heun, S.; Mahr, R. F.; Scherf, U.; Hopmeier, M.; Siegner, U.; Göbel, E. O.; Müllen, K.; Bässler, H. *Chem. Phys. Lett.* **1995**, *240*, 373. (b) Samuel, I. D. W.; Rumbles, G.; Collison, C. J. *Phys. Rev. B* **1995**, *52*, 11573. (c) Webster, S.; Batchelder, D. N. *Polymer* **1996**, *37*, 13713. (d) Gomes da Costa, P.; Conwell, E. M. *Phys. Rev. B* **1993**, *48*, 1993. (e) Brédas, J. L.; Street, G. B. *Acc. Chem. Res.* **1985**, *18*, 309. (f) Su, W. P.; Schrieffer, J. R.; Heeger, A. J. *Phys. Rev. Lett.* **1979**, *42*, 1698. (g) Conil, J.; Beljonne, D.; Heller, C. M.; Campbell, I. H.; Laurich, B. K.; Smith, D. L.; Bradley, D. D. C.; Müllen, K.; Brédas, J. L. *Chem. Phys. Lett.* **1997**, *278*, 139.

systems. Further control of this dimerization should be possible, for example, by introducing additional weak interactions such as hydrogen bonding and static attraction/repulsion between the dendrons, the subject of future work.

**Acknowledgment.** This work was financially supported by the Zentrum für Multifunktionelle Werkstoffe und Miniaturisierte Funktionseinheiten (BMBF 03N 6500), the Deutsche Forschungsgemeinschaft (Schwerpunkt Feldeffekt transistoren), as well as the EU projects DISCEL (G5RD-CT-2000-00321) and MAC-Mes (Grd2-2000-30242). We thank Christine

Rosenauer for the DLS measurements. M. Kastler thanks “Fonds der Chemischen Industrie” and the “Bundesministerium für Bildung und Forschung” for financial support.

**Supporting Information Available:** The synthesis and characterization of all of the new compounds and additional  $^1\text{H}$  NMR spectra of compounds **1**, **2a**, and **2b** under different conditions. This material is available free of charge via the Internet at <http://pubs.acs.org>.

JA047577R